Lyapunov-based Model Predictive Control of Particulate Processes Subject to Asynchronous Measurements

Jinfeng Liu, David Muñoz de la Peña, Panagiotis D. Christofides and James F. Davis

Abstract— This work focuses on state feedback model predictive control of particulate processes subject to asynchronous measurements. A population balance model of a typical continuous crystallizer is taken as an application example. Three controllers, a standard model predictive controller and two recently proposed Lyapunov-based model predictive controllers, are applied to stabilize the crystallizer at an open-loop unstable steady-state in the presence of asynchronous measurements. The stability and robustness properties of the closed-loop system under the three controllers are compared extensively under two different assumptions on how the measurements from the crystallizer are obtained.

I. INTRODUCTION

Particulate processes play a key role in the manufacturing of many chemical products. Examples include the crystallization of proteins for pharmaceutical applications, the emulsion polymerization for the production of latex, and the titania powder aerosol reactors used in the production of white pigments. It is now widely recognized that particulate processes present a number of processing challenges which are not encountered in gas phase or liquid phase processes. One of these challenges is to operate a particulate process in a way that it consistently makes products with a desired particle size distribution (PSD) which is an important quality index of a particulate product. For example, the shape of the crystal size distribution in crystallization processes strongly affects crystal function and downstream processing such as filtration, centrifugation and milling [1].

Population balance modeling is becoming more and more important in particulate processes because it provides a natural framework for the mathematical modeling of particle size distributions (PSDs) (see, for example, the tutorial article [2] and the review article [3]) and has been successfully applied to describe PSDs in many particulate processes. Population balance modeling of particulate processes typically leads to systems of nonlinear partial integro-differential equations that describe the rate of change of the PSD which does not allow their direct use for the synthesis of low-order (and therefore, practically implementable with available computers) nonlinear feedback controllers, see [4].

Jinfeng Liu, Panagiotis D. Christofides and James F. Davis are with the Department of Chemical and Biomolecular Engineering, University of California, Los Angeles, CA 90095-1592, USA. Panagiotis D. Christofides is also with the Department of Electrical Engineering, University of California, Los Angeles, CA 90095-1592, USA. David Muñoz de la Peña is with the Departamento de Ingeniería de Sistemas y Automática, Universidad de Sevilla, Camino de los Descubrimientos S/N, Sevilla 410092, Spain, jinfeng@ucla.edu, davidmps@cartuja.us.es, pdc@seas.ucla.edu, jdavis@conet.ucla.edu.

To overcome this problem, earlier work of our group took advantage of the property that the dominant dynamic behavior of many particulate process models is low-dimensional and proposed [5] a model reduction procedure. This procedure is based on a combination of the method of weighted residuals and the concept of approximate inertial manifold, which leads to the construction of low-order ordinary differential equation (ODE) systems that accurately reproduce the dominant dynamics of broad classes of particulate process models. These ODE systems were subsequently used for the synthesis of nonlinear [5], [6], [4], robust [7], [8] and predictive [9], [10] controllers that enforce desired stability, performance, robustness and constraint handling properties in the closed-loop system. The reader may refer to [11], [12], [13] for reviews of results on simulation and control of particulate processes.

All of the above results on controller design for particulate processes is based on the assumption of continuous sampling and perfect communication between the sensor and the controller. However, one may encounter measurement sample loss, intermittent failures associated with measurement techniques as well as data packet losses over communication networks. Previous work on control subject to actuator/sensor faults has extensively focused on lumped parameter systems. In a recent work [14], a Lyapunov-based nonlinear controller was designed in the presence of input constraints to stabilize a continuous crystallizer subject to asynchronous sensor data losses. This work assumes that a controller is designed under the assumption of continuous measurements, and then, the robustness properties of the closed-loop system under data losses or actuator/sensor faults are studied.

In the present work, we apply nonlinear model predictive control to a continuous crystallization process subject to asynchronous measurement sampling. Asynchronous measurement sampling may arise due to measurement system malfunctions or different sampling rates of the measurement sensors. In particular, a standard model predictive controller, a Lyapunov-based model predictive controller proposed in [15], and a Lyapunov-based model predictive controller developed in our recent work [16] which is designed taking into account explicitly data losses and asynchronous measurements, are applied to stabilize the continuous crystallizer at an open-loop unstable steady-state. Extensive simulations are presented to evaluate the closed-loop stability and robustness of the three control methods under two different assumptions on how the measurements from the crystallizer are obtained.

TABLE I

PROCESS PARAMETERS OF THE CONTINUOUS CRYSTALLIZER

c_s	=	980.2	$kg\ m^{-3}$
c_{0s}	=	999.943	$kg\ m^{-3}$
ρ	=	1770.0	$kg\ m^{-3}$
τ	=	1.0	hr
k_1	=	5.065×10^{-2}	$mm\ m^3\ kg^{-1}\ hr^{-1}$
k_2	=	7.958	$mm^{-3}\ hr^{-1}$
k_3	=	1.217×10^{-3}	

II. MODEL OF A CONTINUOUS CRYSTALLIZER

In this section the population balance model of a continuous crystallizer and the corresponding reduced-order moments model are introduced.

A. Population Balance Model

Under the assumptions of isothermal operation, constant volume, mixed suspension, nucleation of crystals of infinitesimal size, and mixed product removal, a dynamic model for a continuous crystallizer can be derived from a population balance for the particle phase and a mass balance for the solute concentration. The resulting model has the following form [17], [18]:

$$
\begin{aligned}
\frac{\partial n}{\partial \bar{t}} &= -\frac{\partial (R(\bar{t})n)}{\partial r} - \frac{n}{\tau} + \delta(r-0)Q(\bar{t}) \\
\frac{dc}{d\bar{t}} &= \frac{(c_0 - \rho)}{\bar{\epsilon}\tau} + \frac{(\rho - c)}{\tau} + \frac{(\rho - c)}{\bar{\epsilon}}\frac{d\bar{\epsilon}}{d\bar{t}}
\end{aligned}
\tag{1}
$$

where $n(r,\bar{t})$ is the number density of crystals of radius $r \in [0,\infty)$ at time $\bar{t}$ in the suspension, τ is the residence time, c is the solute concentration in the crystallizer, c_0 is the solute concentration in the feed, $\bar{\epsilon} = 1 - \int_0^\infty n(r,\bar{t})\frac{4}{3}\pi r^3 dr$ is the volume of liquid per unit volume of suspension, $R(\bar{t})$ is the growth rate, $\delta(r-0)$ is the standard Dirac function and $Q(\bar{t})$ is the nucleation rate. The term $\delta(r-0)Q(\bar{t})$ accounts for the production of crystals of infinitesimal (zero) size via nucleation. $R(\bar{t})$ and $Q(\bar{t})$ are assumed to follow McCabe's growth law and Volmer's nucleation law, respectively; that is:

$$
R(\bar{t}) = k_1(c - c_s), \ \ Q(\bar{t}) = \bar{\epsilon}k_2 \exp\left[-k_3/(c/c_s - 1)^2\right]
\tag{2}
$$

where k_1, k_2, and k_3 are positive constants and c_s is the concentration of solute at saturation.

The values of the parameters in Eqs. 1 and 2 that define the process studied in this work are given in Table I. The open-loop crystallizer model exhibits a highly oscillatory behavior, which is the result of the interplay between growth and nucleation caused by the relative nonlinearity of the nucleation rate as compared to the growth rate. See [5] for a detailed discussion on the nature of the oscillations exhibited by this process. The population model introduced provides a good approximation of the dynamics of a continuous crystallizer [4]. All simulations have been carried out using the model of Eq. 1.

B. Reduced-order Moments Model

The population balance model is not appropriate for synthesizing model-based low-order feedback control laws due to its distributed parameter nature. To overcome this problem, following the same approach as in [5], we derive a reduced-order moments model which accurately reproduces the dominant dynamics of the system. We define the jth moment of $n(r,\bar{t})$ as:

$$
\mu_j = \int_0^\infty r^j n(r,\bar{t})dr, \ \ j = 0,1,\ldots\infty
\tag{3}
$$

Multiplying the population balance in Eq. 1 by r^j, integrating over all particle sizes, and introducing the following set of dimensionless variables and parameters:

$$
\begin{aligned}
&\tilde{x}_0 = 8\pi\sigma^3\mu_0, \ \tilde{x}_1 = 8\pi\sigma^2\mu_1, \\
&\tilde{x}_2 = 4\pi\sigma\mu_2, \ \tilde{x}_3 = \frac{4}{3}\pi\mu_3, ..., \\
&t = \frac{\bar{t}}{\tau}, \ \sigma = k_1\tau(c_{0s} - c_s), \ Da = 8\pi\sigma^3 k_2\tau, \\
&F = \frac{k_3 c_s^2}{(c_{0s} - c_s)^2}, \ \alpha = \frac{(\rho - c_s)}{(c_{0s} - c_s)}, \\
&\tilde{y} = \frac{(c - c_s)}{(c_{0s} - c_s)}, \ u = \frac{(c_0 - c_{0s})}{(c_{0s} - c_s)}
\end{aligned}
\tag{4}
$$

where c_{0s} is the steady-state solute concentration in the feed, the dominant dynamics of Eq. 1 can be adequately captured by the following fifth-order moments model which includes the dynamics of the first four moments and those of the solute concentration:

$$
\begin{aligned}
\frac{d\tilde{x}_0}{dt} &= -\tilde{x}_0 + (1 - \tilde{x}_3)Da\, e^{\frac{-F}{\tilde{y}^2}} \\
\frac{d\tilde{x}_1}{dt} &= -\tilde{x}_1 + \tilde{y}\tilde{x}_0 \\
\frac{d\tilde{x}_2}{dt} &= -\tilde{x}_2 + \tilde{y}\tilde{x}_1 \\
\frac{d\tilde{x}_3}{dt} &= -\tilde{x}_3 + \tilde{y}\tilde{x}_2 \\
\frac{d\tilde{y}}{dt} &= \frac{1 - \tilde{y} - (\alpha - \tilde{y})\tilde{y}\tilde{x}_2}{1 - \tilde{x}_3} + \frac{u}{1 - \tilde{x}_3}
\end{aligned}
\tag{5}
$$

where $\tilde{x}_\nu$, $\nu = 0,1,2,3$, are dimensionless moments of the crystal size distribution, $\tilde{y}$ is the dimensionless concentration of the solute in the crystallizer and u is a dimensionless concentration of the solute in the feed. The values of the dimensionless model parameters in Eq. 4 are given in Table II. Note that since the moments of order four and higher do not affect those of order three and lower, the state of the infinite dimensional system is bounded when $\tilde{x}_3$ and $\tilde{y}$ are bounded, and it converges to a globally exponentially stable equilibrium point when $\lim_{t\to\infty} \tilde{x}_3 = c_1$ and $\lim_{t\to\infty} \tilde{y} = c_2$, where c_1, c_2 are constants. The state of the crystallizer is denoted as $\tilde{x} = [\tilde{x}_0\ \tilde{x}_1\ \tilde{x}_2\ \tilde{x}_3\ \tilde{y}]^T$.

The reduced-order moments model is a very good approximation of the population balance model and is suitable for directly synthesizing model-based low-order feedback

σ	=	$k_1\tau(c_{0s}-c_s)$	=	1.0	mm
Da	=	$8\pi\sigma^3 k_2\tau$	=	200.0	
F	=	$k_3 c_s^2/(c_{0s}-c_s)^2$	=	3.0	
α	=	$(\rho - c_s)/(c_{0s}-c_s)$	=	40.0	

control laws. The reader may refer to [5], [8] for a detailed derivation of the moments model, and to [4] for further results and references in this area.

The stability properties of the fifth-order model of Eq. 5 have been studied and it has been shown [18] that the global phase space of this model has a unique unstable steady-state $\tilde{x}_s = [\tilde{x}_{0s}\ \tilde{x}_{1s}\ \tilde{x}_{2s}\ \tilde{x}_{3s}\ \tilde{y}_s]^T$ surrounded by a stable periodic orbit at

$$\tilde{x}_s = [0.0471\ 0.0283\ 0.0169\ 0.0102\ 0.5996]^T,$$

and that the linearization of Eq. 1 around the unstable steady-state includes two isolated complex conjugate eigenvalues with a positive real part. The control objective is to regulate the system to the unstable steady state $\tilde{x}_s$ by manipulating the solute feed concentration c_0.

We consider constraints in the input. The dimensionless solute feed concentration, u, is subject to the constraints: $-u_{max} \leq u \leq u_{max}$, where $u_{max} = 3$. For $u_{max} = 3$, the constraint on the inlet solute concentration corresponds to $940\ kg/m^3 \leq c_0 \leq 1060\ kg/m^3$.

We define x as the deviation of the state of the system $\tilde{x}$ from the steady-state $\tilde{x}_s$; that is $x = \tilde{x} - \tilde{x}_s$. Using Eq. 5, the dynamics of x can be written in the following compact form:

$$\dot{x}(t) \quad = \quad f(x(t)) + g(x(t))u(t) \tag{6}$$

where $x = [x_0\ x_1\ x_2\ x_3\ y]^T$.

Next we are going to define a feedback control law $h_L : R^n \rightarrow R$ which satisfies $h_L(0) = 0$ that renders the origin $x = 0$ of the closed-loop system of Eq. 6 asymptotically stable under continuous measurements. Stabilizing state feedback control laws for nonlinear systems have been developed using Lyapunov techniques; the reader may refer to [19], [20] for results on this area. In this work we use the Lyapunov-based feedback control proposed in [21] (see also [22], [23]) which is based on a control Lyapunov function of the open-loop system.

Consider the control Lyapunov function $V(x) = x^T P x$ with $P = I$ for the system of Eq. 6. The following Lyapunov-based feedback control law [21] asymptotically stabilizes the open-loop unstable steady-state under continuous state feedback implementation for an appropriate set of initial conditions:

$$h_L(x) = -k(x)L_g V(x) \tag{7}$$

where $k(x)$ is equal to

$$\begin{cases} 0, \ \text{if } L_g V(x) = 0 \\ \dfrac{L_f V(x) + \sqrt{(L_f V(x))^2 + (u_{max}L_g V(x))^4}}{(L_g V(x))^2 \left[1 + \sqrt{1 + (u_{max}L_g V(x))^2}\right]}, \ \text{else} \end{cases}$$

with $L_f V(x) = \dfrac{\partial V(x)}{\partial x} f(x)$ and $L_g V(x) = \dfrac{\partial V(x)}{\partial x} g(x)$. The feedback controller $h_L(x)$ will be used to design the contractive constraints of the two Lyapunov-based model predictive controllers which will be presented in Section IV

III. MODELING ASYNCHRONOUS MEASUREMENTS

Most control systems assume that the measurements from the sensors are obtained in a continuous periodic pattern and that the communications between the different components of the system are flawless. However, in many processes these assumptions do not hold due to a host of measurements difficulties and possible errors in the communications (for example if wireless links are used to implement the control system). In this case, the system is subject to asynchronous measurements. Measuring the concentration and the properties of the PSD of a continuous crystallizer is a difficult task that might take a variable time. We assume that the sampling of the state of the continuous crystallizer of Eq. 1 takes at least 15 minutes, and if errors occur in the sampling system or in the communication network, it may take a much longer time. We assume that the maximum time interval (worst case occurrence) between two consecutive measurements is shorter than 2.5 hours, which is denoted as T_{max}. In Section V we present simulation results under two different assumptions on how the measurements from the crystallizer are obtained. In this section, we present how we model sampled-data systems subject to asynchronous measurements.

To account for asynchronous sampling, the sampling times are defined by an increasing time sequence $\{t_{k\geq0}\}$. At each sampling time t_k, a new measurement from the sensors is obtained. The interval between two consecutive samplings is not fixed. In the simulation section, we present two different ways of generating the time sequence $\{t_{k\geq0}\}$. The only assumption made on the time sequence $\{t_{k\geq0}\}$ is that there is an upper bound (which is T_{max}) on the maximum time in which the system operates in open-loop. This bound on the maximum period of time in which the loop is open has been also used in other works in the literature [24], [25], [26], [27] and is needed in the present stabilization problem because the open-loop crystallizer is unstable.

In this paper we also take into account that the controller may not receive the whole state (x_0, x_1, x_2, x_3, y) at each sampling instant but just part of it; that is, the PSD measurement x_0, x_1, x_2, x_3 or the solute concentration measurement y (see Fig. 1-2). This is due to the fact that PSD and solute concentration are measured by different sensors with different sampling rates. At sampling time t_k, if only part of the state is available, an estimation of the current state $\hat{x}(t_k)$ is obtained and sent to the controller to generate a new control input. We use an auxiliary variable $s(t_k)$ to indicate what part of the process state is available at sampling time t_k as follows:

1) $s(t_k) = 1$ implies that both measurements of PSD and solute concentration are available at t_k, and $\hat{x}(t_k) = x(t_k)$.

2) $s(t_k) = 2$ implies that only the measurement of PSD is available at t_k. The corresponding value of the solute concentration at t_k is estimated by using the last available value of solute concentration; that is, $\hat{y}(t_k) = \hat{y}(t_{k-1})$.

3) $s(t_k) = 3$ implies that only the measurement of solute concentration is available at t_k. The corresponding state of PSD at t_k is estimated by the reduced-order moments model of Eq. 6.

The estimated state used by the controller at each sampling time $\hat{x}(t_k)$ is given by the following equation:

$$
\begin{cases}
x(t_k) & \text{if } s(t_k) = 1 \\
\{x_0(t_k), x_1(t_k), x_2(t_k), x_3(t_k), \hat{y}(t_{k-1})\} & \text{if } s(t_k) = 2 \\
\{\hat{x}_0(t_k), \hat{x}_1(t_k), \hat{x}_2(t_k), \hat{x}_3(t_k), y(t_k)\} & \text{if } s(t_k) = 3
\end{cases}
\tag{8}
$$

where $\hat{x}_\nu, \nu = 0, 1, 2, 3$, are estimated by using the reduced-order moments model. Note that we have to store the implemented manipulated input trajectory.

In this class of processes, the solute concentration is obtained with a higher sampling rate than the crystallizer PSD. This motivates using the last available value of the solute concentration when a new PSD measurement is obtained. On the other hand, instead of using the last available values of the PSD each time we obtain a new concentration measurement, which may introduce a large error because the PSD is sampled less frequently, we use the reduced-order moments model to estimate the missing information, which increases the computational complexity but decreases the estimation error.

The controller has to take into account that the measurements arrive in an asynchronous manner and that the time in which it has to operate in open-loop may be long. In order to decide the manipulated input $u(t)$ that has to be applied at each time t, the controller uses the last estimated state $\hat{x}(t_k)$ and the corresponding sampling time t_k. We assume that each controller is defined by a function $h(\Delta, \hat{x}(t_k))$, where $\hat{x}$ is the last available estimated state and Δ is the time that has passed since that state was received. This function allows us to model different implementation strategies.

In order to consider the models in this work in a unified time scale and with the same manipulated input, we substitute Eq. 2, the expressions of dimensionless time t and manipulated input u into Eq. 1. We obtain the following asynchronous nonlinear model for the closed-loop system of the crystallizer:

$$
\begin{aligned}
\frac{1}{\tau}\frac{\partial n}{\partial t} &= -k_1(c - c_s)\frac{\partial n}{\partial r} - \frac{n}{\tau} \\
&\quad + \delta(r - 0)\bar{\epsilon}k_2 \exp\left[-k_3/(c/c_s - 1)^2\right] \\
\frac{1}{\tau}\frac{dc}{dt} &= \frac{(c_{0s} - \rho)}{\bar{\epsilon}\tau} + \frac{(\rho - c)}{\tau} \\
&\quad + \frac{(\rho - c)}{\bar{\epsilon}\tau}\frac{d\bar{\epsilon}}{dt} + \frac{(c_{0s} - c_s)u(t)}{\bar{\epsilon}\tau}, \ t \in [t_k, t_{k+1}] \\
u(t) &= h(t - t_k, \hat{x}(t_k))
\end{aligned}
\tag{9}
$$

At time t_k, new information is available from the sensors and the content of the information is decided by the corresponding value of $s(t_k)$. The state $\hat{x}(t_k)$ is an estimation of the actual state $x(t_k)$ and it is estimated by the approach presented before in this section, see Eq. 8. The controller generates a future manipulated input trajectory $h(\Delta, \hat{x})$ that depends on this estimated state, where Δ is the time that has passed since t_k.

IV. Model Predictive Control

Model predictive control (MPC) is a popular control strategy based on using a model of the process to predict at each sampling time, the future evolution of the system from the current state along a given prediction horizon. Using these predictions, the manipulated input trajectory that minimizes a given performance index is computed solving a suitable optimization problem. To obtain finite-dimensional optimization problems, MPC optimizes over the family of piecewise constant trajectories with a fixed sampling time and a fixed prediction horizon (i.e., a fixed length). This implies that the MPC controllers are implemented in a sample and hold scheme. The MPC framework is particularly appropriate for controlling systems subject to asynchronous measurements because the actuator can profit from the predicted evolution of the system, to update the manipulated input when feedback is lost, instead of setting the manipulated input to a fixed value (normally to zero or to the last implemented manipulated input). In this section, three different MPC controllers, a standard model predictive controller and two recently proposed Lyapunov-based model predictive controllers are introduced. These controllers are based on the reduced-order moments model of Eq. 6 and the Lyapunov-based controller of Eq. 7 presented in Section II.

A. Standard Model Predictive Control

The standard MPC controller used in this paper is based on the following optimization problem [28]:

$$
\begin{aligned}
\min_{u(\tau) \in S(\Delta_c)} & \quad \int_0^{N\Delta_c}[x(\tau)^T Q_c x(\tau) + u(\tau)^T R_c u(\tau)]d\tau \\
\text{s.t.} & \quad \dot{x}(\tau) = f(x(\tau)) + g(x(\tau))u(\tau) \\
& \quad x(0) = \hat{x} \\
& \quad |u(\tau)| \leq u_{max}, \ \forall \tau \in [0, N\Delta_c]
\end{aligned}
\tag{10}
$$

where $S(\Delta_c)$ is the family of piece-wise constant functions with sampling period Δ_c, $x(\tau)$ is the predicted trajectory of the system by the reduced-order moments model for the manipulated input trajectory computed by the MPC, Q_c, R_c are positive definite weight matrices that define the cost, $\hat{x}$ is the initial condition and u_{max} is the bound on the control action.

The initial state is provided as a parameter to the MPC optimization problem. When at a given time step, a new estimate of the actual state $\hat{x}$ is obtained, the optimization problem defined in Eq. 10 is solved to obtain the corresponding optimal manipulated input trajectory $u^*(\tau)$ of length $N\Delta_c$. Usually, only the first move of the trajectory ($u(\tau) \in [0, \Delta_c]$) is used. This is the standard receding horizon strategy and it does not take into account that the state might be not available at a given sampling time

due to data losses or asynchronous measurement sampling. The control law corresponding to the MPC controller that takes into account asynchronous measurements is defined as follows:

$$h(\Delta, \hat{x}) = u^*(\Delta)$$

where u^* is the solution of the optimization problem defined in Eq. 10 for an initial state $x(0) = \hat{x}$. Note that this control law is not defined for all times. The optimal trajectory u^* is of length $N\Delta_c$. This limits the maximum time in which the MPC controller can operate in open-loop.

B. Lyapunov-based Model Predictive Control I

The standard MPC controller used in this work is based on minimizing a given cost function defined by matrices Q_c and R_c, using the reduced-order moments model subject to constraints on the input. No additional constraints are used to guarantee closed-loop stability properties. In order to guarantee the stability and robustness of the closed-loop system, the MPC optimization problem has to be modified. In this subsection we present the Lyapunov-based model predictive controller (LMPC) proposed in [15]. This controller guarantees practical stability of the closed-loop system under the assumption of synchronous measurements and no measurement unavailability. This controller is based on the previously designed Lyapunov-based controller h_L that guarantees asymptotic stability of the closed-loop system under continuous measurements. This controller is used to define a contractive constraint which guarantees that the LMPC inherits the stability and robustness properties of the Lyapunov-based controller. The controller introduced in [15] is based on the following optimization problem:

$$\min_{u(\tau) \in S(\Delta_c)} \int_0^{N\Delta_c} [x(\tau)^T Q_c x(\tau) + u(\tau)^T R_c u(\tau)]d\tau \quad \text{(11a)}$$

$$\text{s.t. } \dot{x}(\tau) = f(x(\tau)) + g(x(\tau))u(\tau) \quad \text{(11b)}$$

$$x(0) = \hat{x} \quad \text{(11c)}$$

$$|u(\tau)| \leq u_{max}, \ \forall \ \tau \in [0, \ N\Delta_c] \quad \text{(11d)}$$

$$\frac{\partial V(\hat{x})}{\partial \hat{x}} f(\hat{x}, u(0)) \leq \frac{\partial V(\hat{x})}{\partial \hat{x}} f(\hat{x}, h_L(\hat{x})) \quad \text{(11e)}$$

The constraint of Eq. 11e guarantees that the value of the time derivative of the control Lyapunov function at the initial evaluation time of the LMPC is lower or equal to the value obtained if the Lyapunov-based controller $u = h_L(x)$ is implemented in the closed-loop system. This is the contractive constraint that allows one to prove (when no measurement unavailability is taken into account) that the LMPC inherits the stability and robustness properties of the Lyapunov-based controller h_L. The corresponding function $h(\Delta, \hat{x})$ is defined as in the MPC case.

C. Lyapunov-based Model Predictive Control II

In this section, the Lyapunov-based model predictive control law developed in [16] is given. This control law takes into account data losses and asynchronous measurements explicitly. In order to present the optimization problem that defines this LMPC, we need the following definition:

Definition 1: The sampled trajectory of Eq. 6 of length $N\Delta_c$ associated with the Lyapunov-based feedback control law $h_L(x)$ with initial state $x_L(0)$ is denoted by $x_L(\tau)$ and is obtained by solving recursively

$$\begin{aligned} \dot{x}_L(\tau) &= f(x_L(\tau)) + g(x_L(\tau))u(\tau_k), \ \tau \in [\tau_k, \tau_{k+1}] \\ u(\tau_k) &= h_L(x_L(\tau_k)) \end{aligned}$$
$$(12)$$

where $\tau_k = k\Delta_c$ and $k = 0, \ldots, N-1$.

The sampled trajectory of Eq. 6 associated with the Lyapunov-based feedback control law $h_L(x)$ is the state trajectory of the crystallizer in closed-loop with the Lyapunov-based controller applied in a sample-and-hold scheme. This state trajectory is used to define the contractive constraint of the following LMPC optimization problem:

$$\min_{u(\tau) \in S(\Delta_c)} \int_0^{N\Delta_c} [x(\tau)^T Q_c x(\tau) + u(\tau)^T R_c u(\tau)]d\tau \quad \text{(13a)}$$

$$\text{s.t. } \dot{x}(\tau) = f(x(\tau)) + g(x(\tau))u(\tau) \quad \text{(13b)}$$

$$x(0) = \hat{x} \quad \text{(13c)}$$

$$|u(\tau)| \leq u_{max}, \ \forall \ \tau \in [0, \ N\Delta_c] \quad \text{(13d)}$$

$$V(x(\tau)) \leq V(x_L(\tau)), \ \forall \ \tau \in [0, \ N\Delta_c] \quad \text{(13e)}$$

where $x_L(\tau)$ is the sampled trajectory of Eq. 6 of Definition 1 for an initial state $x_L(0) = \hat{x}$.

The main difference between the LMPC of Eq. 13 and the LMPC of Eq. 11 presented in last subsection is the contractive constraint. The constraint of Eq. 11e guarantees that the LMPC controller of Eq. 11 provides at least the same decrease of the control Lyapunov function as the Lyapunov-based controller in the first time step. When data losses or asynchronous measurements are taken into account, in order to prove that the LMPC of Eq. 13 inherits the same properties of the Lyapunov-based controller, the contractive constraint of Eq. 13e must hold along the whole prediction horizon. In this manner, when measurements are unavailable, the optimal manipulated input trajectory evaluated guarantees that the predicted decrease of the control Lyapunov function is at least equal to the one obtained applying the Lyapunov-based controller. The corresponding function $h(\Delta, \hat{x})$ is defined as in the MPC case.

Note that the three model predictive controllers presented in this section assume a given sampling time Δ_c. In most control systems where the measurements are obtained synchronously and the communications are flawless, this sampling time is equal to the sampling time used to obtain new measurements and implement the manipulated input (sample-and-hold schemes). In this paper, however, we deal with systems subject to asynchronous measurements. This implies that and the time sequence that determines when new information is available is independent of Δ_c.

D. MPC Parameters

We denote, in the remainder of this work, the three model predictive controllers of Eqs. 10, 11 and 13 as MPC, LMPC I and LMPC II, respectively. The cost functions of these controllers are defined by matrices $Q_c = P$ and $R_c = 4$. The weight matrices Q_c and R_c have been chosen to provide a
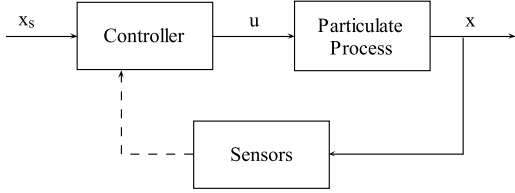
Fig. 1. Closed-loop system with asynchronous measurements: the whole state is sampled simultaneously.

Fig. 2. Closed-loop system with asynchronous measurements: the states of PSD and solute concentration are sampled separately.

Fig. 3. Asynchronous sampling times for both PSD and solute concentration.

performance similar to the Lyapunov-based controller under a sample-and-hold implementation. The sampling time of the MPC controllers is $\Delta_c = 0.25h$ which is equal to the minimum time needed to obtain a new measurement.

Through simulations, we have estimated the transition time for the crystallizer in closed-loop with the Lyapunov-based controller which is 2 hours for states x_0, y and 4 hours for states x_1, x_2, x_3. We choose the prediction horizon $N = 11$ for the model predictive controllers so that the prediction captures most of the dynamic evolution of the process.

V. SIMULATION RESULTS

In this section, we apply the three model predictive control laws MPC, LMPC I and LMPC II to the continuous crystallizer population balance model of Eq. 9 to evaluate the stability and robustness properties of the corresponding closed-loop systems in the presence of asynchronous measurements. First, we simulate the system with asynchronous measurements in which measurements of PSD and solute concentration come simultaneously (see Fig. 1), and then simulate with asynchronous measurements in which PSD and solute concentration are sampled separately (see Fig. 2). The control objective is to suppress the oscillatory behavior of the crystallizer and stabilize it at the open-loop unstable steady-state $\tilde{x}_s$ that corresponds to the desired PSD by manipulating the solute feed concentration. The following initial conditions are used in the simulations:

$$n(0, r) = 0.0, \ c(0) = 990.0 \ kg \ m^{-3},$$
$$\tilde{x}(0) = [0 \ 0 \ 0 \ 0 \ 0.498]^T. \tag{14}$$

To simulate the continuous crystallizer, we use a second-order accurate finite-difference discretization scheme. At every model evaluation step (which is different from the sampling time and should be chosen to be sufficiently small in order to get a continuous and accurate solution) of Eq. 9, the values of $n(t, r)$ and $c(t)$ can be obtained, so we can use them to calculate the state x at that time using Eqs. 3 and 4 and the steady-state $\tilde{x}_s$.

A. PSD and Solute Concentration Sampled Simultaneously

For the simulations in this subsection, we assume that the time between consecutive measurements is obtained using a random process and that the PSD and solute concentration are measured simultaneously. To generate the time intervals between samples we use a random Poisson process as in [29], [14]. The Poisson process is defined by the number of events per unit time W. At a given time t, an event
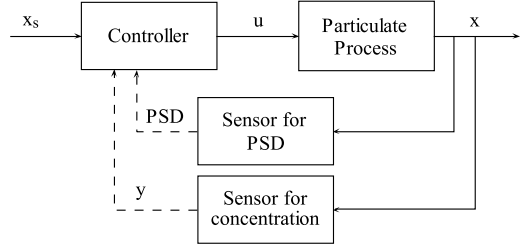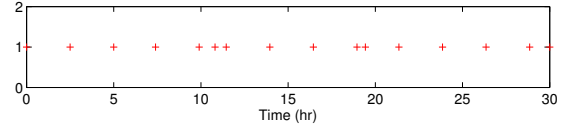
takes place which means that the state is sampled. The interval between two consecutive sampling times is given by $\Delta_a = \frac{-ln\chi}{W}$, where χ is a random variable with uniform probability distribution between 0 and 1. At $t + \Delta_a$, another event occurs. The sequence $\{t_{k \geq 0}\}$ and the corresponding auxiliary variable $s(t_k)$ for a simulation of length t_{sim} is generated as follows:

$t_0 = 0, \ k = 0$
while $t_k < t_{sim}$
    $\chi = rand(1)$
    $t_{k+1} = t_k + \frac{-ln\chi}{W}$
    if $t_{k+1} > t_k + T_{max}$, then $t_{k+1} = t_k + T_{max}$
    if $t_{k+1} < t_k + T_{min}$, then $t_{k+1} = t_k + T_{min}$
    $s(t_k) = 1, \ k = k + 1$
end

where $rand(1)$ generates a uniformly distributed random value χ between 0 and 1, T_{max} is the maximum allowable transmission interval and T_{min} is the minimum time interval between two consecutive samplings. Note that T_{min} should be smaller than T_{max}; that is, $T_{min} < T_{max}$. As mentioned before T_{max} is $2.5hr$. The minimum time limit T_{min} is equal to the synchronous sampling time, that is $T_{min} = \Delta_m = 0.25hr$. For the simulations carried out in this subsection we pick the value of the number of events per unit time to be $W = 0.15$. The sampling times for the simulations are shown in Fig. 3. Note that because the number of events is low, the time between consecutive samplings (and hence, the time in which the control system must operate in open-loop) may be large but always smaller than T_{max}.

First, we compare LMPC II with MPC. The state and manipulated input trajectories of this simulation are shown in Fig. 4. In this simulation, MPC can not stabilize the process, while LMPC II is able to maintain the process at the desired steady-state. Second, we compare LMPC II with LMPC I. The state and manipulated input trajectories are shown in Fig. 5. Though LMPC II and LMPC I can both stabilize
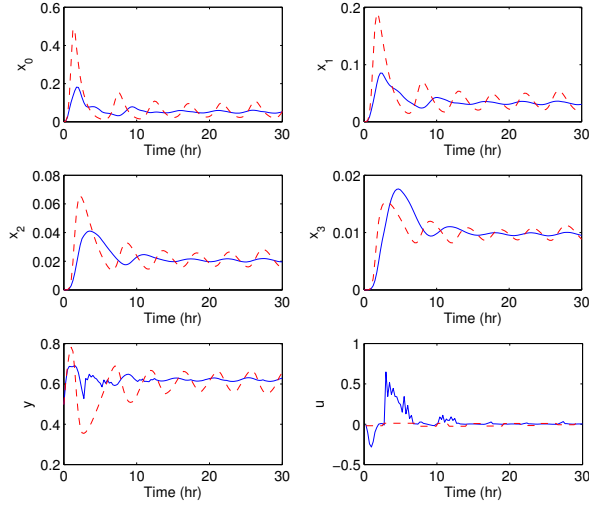
Fig. 4. State and manipulated input trajectories of Eq. 9 with PSD and solute concentration sampled asynchronously and simultaneously using the predicted manipulated input trajectories of LMPC II of Eq. 13 (solid curves) and MPC of Eq. 10 (dashed curves).

Fig. 5. State and manipulated input trajectories of Eq. 9 with PSD and solute concentration sampled asynchronously and simultaneously using the predicted manipulated input trajectories of LMPC II of Eq. 13 (solid curves) and LMPC I of Eq. 11.

the process, the transient of the closed-loop system under LMPC II is shorter than the transient under LMPC I and has a smaller overshoot.

From the results of this subsection, one can conclude that LMPC II using the predicted manipulated input trajectory is the most robust in the presence of asynchronous sampling among the three controllers.

B. PSD and Solute Concentration Sampled Separately

For this set of simulations, we assume that we have the measurements of PSD and solute concentration sampled separately. This implies that we may get a measurement of PSD at a sampling time but lack corresponding measurement of solute concentration; and we may have a measurement of solute concentration but lack the corresponding measurement of PSD. In addition, we have asynchronous sampling which means that the length of the time interval between two consecutive measurements is varying.

Using the same method presented in Section V-A, we generate two different time sequences $\{t_{k\geq0}^p\}$ for PSD ($s = 2$) and $\{t_{k\geq0}^c\}$ for solute concentration ($s = 3$) using $W^p = 0.15$ and $W^c = 1$, respectively. Both time sequences are generated with the same constraints $T_{max} = 2.5hr$ and $T_{min} = 0.25hr$. The choice of $W^c = 1$ for $\{t_{k\geq0}^c\}$ is based on the fact that we can get a measurement of concentration faster. The two sequences are merged into an ordered one $\{t_{k\geq0}\}$ by increasing time and the overlapping times correspond to instants that both measurements of PSD and solute concentration can be obtained ($s = 1$). The sampling sequence $\{t_{k\geq0}\}$ is shown in Fig. 6. Every sampling instant in the new sequence represents a measurement of PSD or solute concentration or both. The auxiliary variable $s(t_k)$ is defined accordingly.
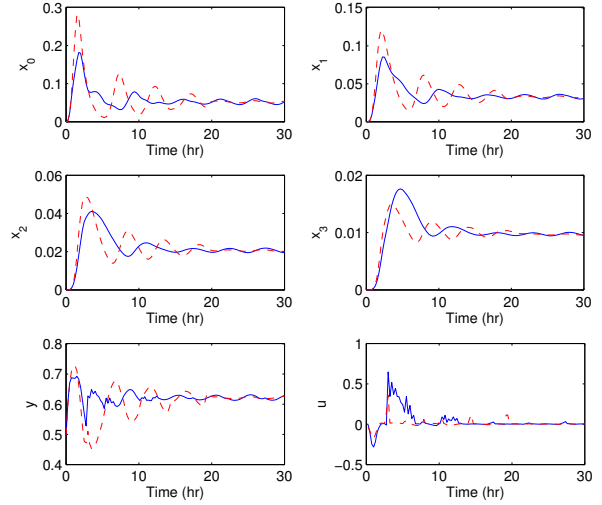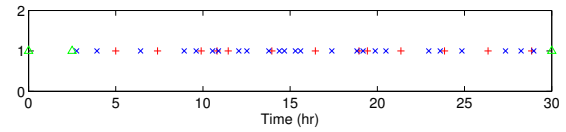
Fig. 6. Asynchronous sampling times, +: sampling times of PSD ($s(t_k) = 2$), ×: sampling times of solute concentration ($s(t_k) = 3$), Δ: sampling times of both PSD and solute concentration ($s(t_k) = 1$).

We first compare LMPC II with MPC. The state and manipulated input trajectories are shown in Fig. 7. As expected, LMPC II is able to stabilize the process, but MPC fails. The result is consistent with the previous simulations. Following that, we compare LMPC II with LMPC I. The state and manipulated input trajectories are shown in Fig. 8. In this figure it can be seen that LMPC I can also stabilize the process but it takes a longer time compared with LMPC II.

Summing up, LMPC II using the predicted manipulated input trajectory yields a more robust closed-loop performance when the process is subject to asynchronous sampling.

VI. CONCLUSION

In this work, a continuous crystallizer was taken as an example to demonstrate the problem of preserving closed-loop stability and robustness of a standard MPC and two recently proposed Lyapunov-based model predictive controllers in the presence of asynchronous measurements. The simulation results demonstrate that the closed-loop system under the LMPC controller that takes into account possible measurement unavailability is more robust with respect to asynchronous measurements.
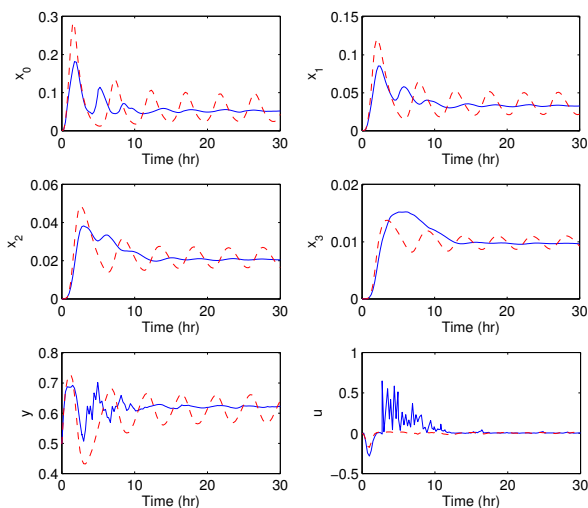
Fig. 7. State and manipulated input trajectories of Eq. 9 with PSD and solute concentration sampled asynchronously and separately using the predicted manipulated input trajectories of LMPC II of Eq. 13 (solid curves) and MPC of Eq. 10 (dashed curves).
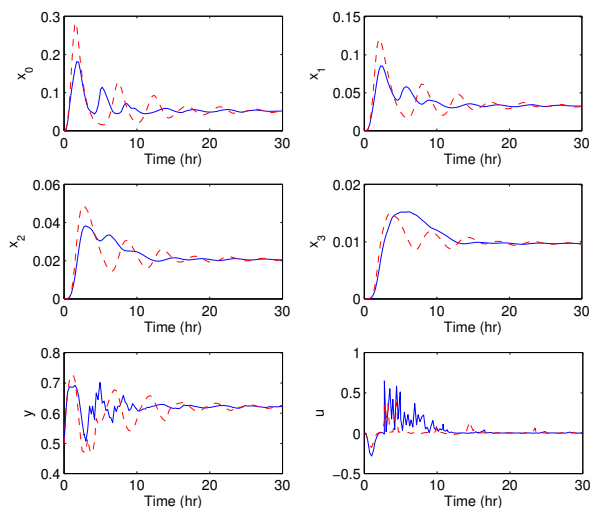
Fig. 8. State and manipulated input trajectories of Eq. 9 with PSD and solute concentration sampled asynchronously and separately using the predicted manipulated input trajectories of LMPC II of Eq. 13 (solid curves) and LMPC I of Eq. 11 (dashed curves).

REFERENCES

[1] J. B. Rawlings, S. M. Miller, and W. R. Witkowski, "Model identification and control of solution crystallization process," *Industrial & Engineering Chemistry Research*, vol. 32, pp. 1275–1296, 1993.

[2] H. M. Hulburt and S. Katz, "Some problems in particle technology: A statistical mechanical formulation," *Chemical Engineering Science*, vol. 19, pp. 555–574, 1964.

[3] D. Ramkrishna, "The status of population balances," *Reviews in Chemical Engineering*, vol. 3, pp. 49–95, 1985.

[4] P. D. Christofides, *Model-based control of particulate processes*. Kluwer Academic Publishers, 2002.

[5] T. Chiu and P. D. Christofides, "Nonlinear control of particulate processes," *AIChE Journal*, vol. 45, pp. 1279–1297, 1999.

[6] A. Kalani and P. D. Christofides, "Nonlinear control of spatially-inhomogeneous aerosol processes," *Chemical Engneering Science*, vol. 54, pp. 2669–2678, 1999.

[7] T. Chiu and P. D. Christofides, "Robust control of particulate processes using uncertain population balances," *AIChE Journal*, vol. 46, pp. 266–280, 2000.

[8] N. H. El-Farra, T. Chiu, and P. D. Christofides, "Analysis and control of particulate processes with input constraints," *AIChE Journal*, vol. 47, pp. 1849–1865, 2001.

[9] D. Shi, P. Mhaskar, N. H. El-Farra, and P. D. Christofides, "Predictive control of crystal size distribution in protein crystallization," *Nanotechnology*, vol. 16, pp. S562–S574, 2005.

[10] D. Shi, N. H. El-Farra, M. Li, P. Mhaskar, and P. D. Christofides, "Predictive control of particle size distribution in particulate processes," *Chemical Engineering Science*, vol. 61, pp. 268–281, 2006.

[11] P. Daoutidis and M. Henson, "Dynamics and control of cell populations," in *AIChE Symposium Series: Proceedings of 6th International Conference on Chemical Process Control*, J. B. Rawlings, Ed., 2002, pp. 274–289.

[12] F. J. Doyle, M. Soroush, and C. Cordeiro, "Control of product quality in polymerization processes," in *AIChE Symposium Series: Proceedings of 6th International Conference on Chemical Process Control*, J. B. Rawlings, Ed., 2002, pp. 290–306.

[13] P. D. Christofides, N. H. El-Farra, M. H. Li, and P. Mhaskar, "Model-based control of particulate processes," *Chemical Engineering Science*, vol. 63, pp. 1156–1172, 2008.

[14] A. Gani, P. Mhaskar, and P. D. Christofides, "Handling sensor malfunctions in control of particulate processes," *Chemical Engineering Science*, vol. 63, pp. 1217–1229, 2008.

[15] P. Mhaskar, N. H. El-Farra, and P. D. Christofides, "Predictive control of switched nonlinear systems with scheduled mode transitions," *IEEE Transactions on Automatic Control*, vol. 50, pp. 1670–1680, 2005.

[16] D. Muñoz de la Peña and P. D. Christofides, "Lyapunov-based model predictive control of nonlinear systems subject to data losses," *IEEE Transactions on Automatic Control, accepted for publication*, 2008.

[17] S. J. Lei, R. Shinnar, and S. Katz, "The stability and dynamic behavior of a continuous crystallizer with a fines trap," *AIChE Journal*, vol. 17, pp. 1459–1470, 1971.

[18] G. R. Jerauld, Y. Vasatis, and M. F. Doherty, "Simple conditions for the appearance of sustained oscillations in continuous crystallizers," *Chemical Engineering Science*, vol. 38, pp. 1675–1681, 1983.

[19] P. Kokotovic and M. Arcak, "Constructive nonlinear control: a historical perspective," *Automatica*, vol. 2001, pp. 637–662, 37.

[20] P. D. Christofides and N. H. El-Farra, *Control of nonlinear and hybrid process systems: Designs for uncertainty, constraints and time-delays*. Berlin, German: Springer-Verlag, 2005.

[21] Y. Lin and E. D. Sontag, "A universal formula for stabilization with bounded controls," *System & Control Letters*, vol. 16, pp. 393–397, 1991.

[22] N. H. El-Farra and P. D. Christofides, "Integrating robustness, optimality and constraints in control of nonlinear processes," *Chemical Engineering Science*, vol. 56, pp. 1841–1868, 2001.

[23] ——, "Bounded robust control of constrained multivariabe nonlinear processes," *Chemical Engineering Science*, vol. 58, pp. 3025–3047, 2003.

[24] P. Mhaskar, A. Gani, C. McFall, P. D. Christofides, and J. F. Davis, "Fault-tolerant control of nonlinear process systems subject to sensor faults," *AIChE Journal*, vol. 53, pp. 654–668, 2007.

[25] G. Walsh, O. Beldiman, and L. Bushnell, "Asymptotic behavior of nonlinear networked control systems," *IEEE Transactions on Automatic Control*, vol. 46, pp. 1093–1097, 2001.

[26] G. Walsh, H. Ye, and L. Bushnell, "Stability analysis of networked control systems," *IEEE Transactions on Control Systems Technology*, vol. 10, pp. 438–446, 2002.

[27] L. A. Montestruque and P. J. Antsaklis, "On the model-based control of networked systems," *Automatica*, vol. 39, pp. 1837–1843, 2003.

[28] C. E. García, D. M. Prett, and M. Morari, "Model predictive control: Theory and practice–a suvey," *Automatica*, vol. 25, pp. 335–348, 1989.

[29] P. Mhaskar, A. Gani, N. H. El-Farra, C. McFall, P. D. Christofides, and J. F. Davis, "Integrated fault-detection and fault-tolerant control of process systems," *AIChE Jounary*, vol. 52, pp. 2129–2148, 2006.